RESEARCH

Progerin mislocalizes myocardin-related transcription factor in Hutchinson–Guilford Progeria syndrome

Ryan von Kleeck[1,2], **Paola Castagnino**[1,3] and **Richard K Assoian**[1,2,3]

[1]Department of Systems Pharmacology and Translational Therapeutics, University of Pennsylvania, Philadelphia Pennsylvania, USA
[2]Center for Engineering MechanoBiology, University of Pennsylvania, Philadelphia, Pennsylvania, USA
[3]Institute of Translational Medicine and Therapeutics, University of Pennsylvania, Philadelphia, Pennsylvania, USA

Correspondence should be addressed to R K Assoian: assoian@pennmedicine.upenn.edu

Abstract

Hutchinson–Guilford Progeria syndrome (HGPS) is a rare genetic disease of premature aging and early death due to cardiovascular disease. The arteries of HGPS children and mice are pathologically stiff, and HGPS mice also display reduced arterial contractility. We recently showed that reduced contractility is an early event in HGPS and linked to an aberrantly low expression of smooth muscle myosin heavy chain (smMHC). Here, we have explored the basis for reduced smMHC abundance and asked whether it is a direct effect of progerin expression or a longer-term adaptive response. *Myh11*, the gene encoding for smMHC, is regulated by myocardin-related transcription factors (MRTFs), and we show that HGPS aortas have a reduced MRTF signature. Additionally, smooth muscle cells (SMCs) isolated from HGPS mice display reduced MRTF nuclear localization. Acute progerin expression in WT SMCs phenocopied both the decrease in MRTF nuclear localization and expression of *Myh11* seen in HGPS. Interestingly, RNA-mediated depletion of MRTF-A in WT SMCs reproduced the preferential inhibitory effect of progerin on *Myh11* mRNA relative to *Acta2* mRNA. Our results show that progerin expression acutely disrupts MRTF localization to the nucleus and suggest that the consequent decrease in nuclear coactivator activity can help to explain the reduction in smMHC abundance and SMC contractility seen in HGPS.

Key Words

- arterial contractility
- smooth muscle
- myosin heavy chain
- *Myh11*
- CArG genes

Introduction

Hutchinson–Gilford Progeria syndrome (HGPS) is a rare premature aging disease (1). About 1 year after birth, HGPS children develop progressive clinical signs of advanced aging such as loss of hair, thinning of the skin, stiff joints, and severely stunted growth (2). Among the most prominent defects is arterial dysfunction, including a dramatic loss of vascular smooth muscle cells (SMCs) from the large arteries, a severely fibrotic arterial microenvironment, and prominent atherosclerotic lesions (2, 3). HGPS children typically die in their teenage years due to heart attack and/or stroke.

The classical form of HGPS is a result of a single nucleotide point mutation in the Lamin A gene (*Lmna*), leading to altered splicing and production of a mutant form of Lamin A termed progerin (4, 5, 6). Compared to normal Lamin A, progerin lacks 50 amino acids near the C-terminus and remains permanently farnesylated. While WT Lamin A is a major component of the nuclear lamina,

https://vb.bioscientifica.com
https://doi.org/10.1530/VB-21-0018
© 2022 The authors
Published by Bioscientifica Ltd

This work is licensed under a Creative Commons Attribution-NonCommercial 4.0 International License.

the defect in the biosynthetic processing of progerin leads to its improper incorporation into the inner nuclear membrane and the formation of an altered nuclear lamina network (2, 7, 8, 9).

Lamin A is thought to be an important component in the transduction of mechanical information from the cytoplasm to the nucleus through its association with the linker of nucleoskeleton and cytoskeleton (LINC) complex (10, 11, 12, 13, 14). The LINC complex is comprised of nesprins and Sad1p, UNC-84 (SUN) proteins. Nesprins bind to the actin cytoskeleton (and intermediate filaments) in the cytoplasm and SUN proteins in the nuclear envelope. SUN proteins, in turn, connect to the lamin A-containing nuclear lamina meshwork. Thus, signals that regulate actomyosin contraction can be transmitted to the nucleus through the LINC complex. Mechanical responses, cytoplasmic-nuclear connections, and the LINC complex are altered in progerin-expressing cells (15, 16). Moreover, forced disruption of the LINC complex by expression of the isolated KASH domain from nesprin-2 reduces cell death of progerin-expressing SMCs in response to biaxial stretch *in vitro* as well as in progerin expressing mice (17).

SMCs comprise the media layer of the large elastic arteries and can undergo a reversible differentiation/de-differentiation called 'phenotypic switching' (18, 19, 20, 21, 22). Healthy, arterial SMCs are normally of a 'contractile' phenotype that regulates blood flow by tonic vasoconstriction and dilation; these SMCs have high expression of the smooth muscle contractile machinery, such as smooth muscle myosin (encoded by *Myh11*), α-smooth muscle actin (encoded by *Acta2*), calponin (encoded by *Cnn*), and SM22α/transgelin (encoded by *Tagln*). However, in response to pathologic stimuli such as arterial injury, contractile SMCs dedifferentiate to a more 'synthetic' state in which they downregulate the expression of the contractile genes and become migratory, proliferative, and remodel the extracellular matrix (ECM), presumably to promote wound healing. These synthetic SMCs can then re-differentiate to the contractile phenotype as part of injury resolution (23). In vascular diseases such as atherosclerosis, phenotypic switching can lead to pathological populations of synthetic SMCs that contribute to arterial stenosis and lesion formation (24, 25, 26).

The genes that mark the differentiated SMC are referred to as 'CArG genes' because their expression is strongly regulated by CArG (CC(A/T-rich)$_6$GG) sites. CArG sites can occur in both 5' flanking and intronic DNA sequences and play an important role in smooth muscle subtype-specific expression of SMC contractile genes such as *Myh11* (18, 27, 28, 29, 30). CArG genes, in turn, are regulated by the serum response factor (SRF) transcription factor and the myocardin transcriptional coactivator family: myocardin and the myocardin-related transcription factors, MRTF-A and MRTF-B (18, 27, 31, 32). Myocardin and the MRTFs are major coactivators of SRF in SMCs. Myocardin is constitutively nuclear, but the transcriptional coactivator activity of MRTFs is regulated by their shuttling between the cytoplasm and nucleus, which in turn is regulated by actin polymerization and changes in cell mechanics (33, 34, 35). Epigenetic histone methylation and acetylation as well as transcriptional repression by Kruppel-like factor-4 (KLF4) also play important roles in modulating SRF-mediated CArG gene expression and SMC differentiation (30, 36, 37).

We recently reported that aortas, carotid arteries, and cultured SMCs from an HGPS mouse model display reduced expression of SMC contractile markers, including *Acta2* and especially *Myh11* (38). Thus, HGPS SMCs have a defective contractile phenotype. However, the molecular basis for this reduced expression and whether the defect reflects a direct effect of progerin or a long-term, adaptive response to its expression remain unclear. In this work, we identify defective MRTF nuclear localization as a molecular phenotype of HGPS and use acute progerin expression to assess its direct vs adaptive effects on *Myh11* gene expression, contractility, and MRTF localization.

Materials and methods

Mice and artery isolation

LMNA$^{G609G/+}$ mice on the C57/BL6 background were generously provided Dr Carlos Lopez-Otin (Universidad de Oviedo, Oviedo, Spain). Mice were genotyped using the followingprimers:forward:AAGGGGCTGGGAGGACAGAG; and reverse: AGCATGCCATAGGGTGGAAGGA, with band sizes of 100 bp for the WT and 240 bp for the LMNA^{G609G} genes. Mice were fed a chow diet *ad libitum*. For HGPS mouse experiments, WT littermate controls were obtained from LMNA$^{G609G/+}$ matings. Arteries were perfused with PBS *in situ* through the left ventricle, and the descending aorta was isolated from the end of the aortic arch to the diaphragm. The isolated aorta was cleaned of excess fat, flash-frozen, and stored at −80°C for protein analysis. Animal protocols were approved by the University of Pennsylvania Institutional Animal Care and Use Committee.

Cell culture, RNAi, and viral infections

Primary mouse SMCs were isolated from the descending aortas of 2-month WT and HGPS male mice and prepared

https://vb.bioscientifica.com
https://doi.org/10.1530/VB-21-0018
© 2022 The authors
Published by Bioscientifica Ltd

This work is licensed under a Creative Commons Attribution-NonCommercial 4.0 International License.

by explant culture as described (39). SMCs were cultured in growth medium (1:1 Dulbecco's modified Eagle's medium (DMEM)/Ham's F-12 supplemented with 2 mM L-glutamine and 20 mM HEPES, pH 7.4) with 20% FBS. Cells were passaged at near confluence with trypsin/EDTA and used between passages 4 and 6.

siRNA-mediated knockdown of MRTF-A in near-confluent WT SMCs was performed using Lipofectamine RNAiMAX Transfection Reagent (ThermoFisher #13778100) in OPTI-MEM with a final siRNA concentration of 300 nM (Origene 223701). A non-specific siRNA provided by the manufacturer was used as the control. After 4 h of siRNA transfection, cells were switched to fresh growth medium. Cells were collected for immunoblot and RT-qPCR analyses 72 h after transfection.

For viral infections of isolated SMCs, a GFP-tagged progerin adenovirus was prepared from pBABE-GFP-progerin (Addgene 17663) by sub-cloning into pENTR/D-TOPO with PCR (Invitrogen K2400-20). The resultant GFP-progerin entry vector was gel-purified (Qiagen 28104) and then cloned into the pAd/CMV/V5-DEST Gateway vector (Invitrogen V493-20). The Gateway vector was transfected into 293A cells, and the cells were collected ~10 days after transfection when lytic plaques were visible. Crude lysate from transfected 293A cells was used to transduce additional 293A cells and amplify and titer the virus. The final GFP-progerin adenovirus was incubated overnight with cultured SMCs at 300–500 MOI, after which time the media was replaced with fresh growth media. The cells were then incubated for an additional 56 h (for a total of 72 h after infection). The efficiency of the adeno-GFP-progerin infection in WT SMCs was ~60% as determined by manual counting of GFP+ vs total (Dapi-stained) cells.

A lentivirus encoding the isolated KASH domain from nesprin-2 as a GFP fusion protein (40) and a GFP control lentivirus were graciously provided by Gregg Gundersen (Columbia University). Approximately 5×10^4 WT or HGPS SMCs were plated in individual wells of a 12-well dish (containing 12-mm glass coverslips) and infected with the GFP-KASH lentivirus or a control GFP lentivirus. After overnight infection, the cell culture medium was changed, and 72 h later the cells were either fixed for immunostaining or lysed in TRIzol reagent for analysis by RT-qPCR. Lentiviral infection efficiency was ~80% as judged by the percentage of WT SMCs expressing the GFP-KASH construct.

Traction force microscopy (TFM)

Traction force microscopy was performed as previously described (38). For GFP-progerin experiments, only cells expressing GFP-progerin, as visualized by green fluorescence, were analyzed for traction force microscopy.

Immunostaining and nuclear–cytoplasmic quantification

WT and HGPS primary aortic SMCs were plated on glass coverslips in fresh growth medium at ~60% confluence and incubated for 24 h before fixation in 3.7% formaldehyde in PBS (1 h at room temperature). Coverslips were blocked and permeabilized for 2 h at room temperature in PBS containing 0.4% Triton X-100, 2% BSA, and 50 mM NH_4Cl. Coverslips were rinsed with PBS and incubated overnight at 4°C with antibodies to MRTF-A (Protein Tech #21166-1-AP; 1:50 dilution) or nesprin-2 (kind gift of Gregg Gundersen, Columbia University; 1:200 dilution) diluted in blocking buffer (PBS containing 0.4% Triton X-100, 2% BSA). Coverslips were washed in blocking buffer three times for 10 min each before incubation (2 h at room temperature) with secondary antibody (Alexafluor-488 chicken anti-Rabbit Santa Cruz #A21441, diluted 1:100 or Alexafluor-594 donkey anti-rabbit Invitrogen A32754, diluted 1:100) in blocking buffer containing Dapi. Coverslips were washed three times for 10 min each in blocking buffer, rinsed in PBS, dipped in water, and mounted using SlowFade Gold anti-fade agent (ThermoFisher #P36930). Fluorescent images were acquired on a Nikon Eclipse inverted phase-contrast microscope and captured on the QI Click Qimaging camera using QCapture Suite Plus software.

Nuclear–cytoplasmic ratios of MRTF-A were calculated using ImageJ. The nuclear boundary was traced based on the Dapi stain, and the tracing was added to the region of interest (ROI) manager. This nuclear tracing was then overlayed on the MRTF-A images, and the mean pixel intensity of MRTF-A in the nucleus was recorded (mean pixel intensity = raw integrated density/area). Then, using a long-exposure of MRTF-A staining to identify cell boundaries, the entire cell area was traced, and total MRTF-A raw integrated density was determined for the entire cell. The nuclear raw integrated density of MRTF-A was subtracted from the total cell raw integrated density to yield the cytoplasmic raw integrated density of MRTF-A. The cytoplasmic raw integrated density was divided by the cytoplasmic area (total cell area – nuclear area) to obtain the mean pixel intensity of MRTF-A in the cytoplasm. Nuclear–cytoplasmic ratios are the mean pixel intensity of MRTF-A in the nucleus divided by the mean pixel intensity of MRTF-A in the cytoplasm. For SMCs infected with GFP-progerin, MRTF-A nuclear localization was quantified only

https://vb.bioscientifica.com
https://doi.org/10.1530/VB-21-0018
© 2022 The authors
Published by Bioscientifica Ltd

This work is licensed under a Creative Commons Attribution-NonCommercial 4.0 International License.

in the cells expressing GFP-progerin as visualized under the green fluorescence channel.

Genome-wide transcript analysis

Differentially expressed genes (DEGs) between 2-month WT and HGPS aortas were obtained from GEO dataset GSE165409. Mapping of the raw sequence files, count normalization, and generation of the initial differential expression results in DESeq2 have been described previously (41). Transcripts having a 1.5× fold change and adjusted *P*-values of <0.001 were subjected to a core analysis with Ingenuity Pathway Analysis (IPA, Qiagen). Default settings were used for all other core analysis parameters. The core analysis included the prioritization of upstream regulators based on enrichment of a regulator's target gene set in the DEGs. For each regulator, IPA tested the directionality of each of the genes in the overlap to infer an activation or inactivation of the regulator (Z-score). We defined putative upstream transcriptional regulators of the DEGs as those having Z-scores >2.0 (activated) or <−2.0 (inhibited).

Statistical analysis

Statistical analysis was performed using Prism Software (GraphPad). The statistical tests used for analysis are identified in the respective figure legends. Note that when immunoblotting results were compiled from independent experiments that were fractionated and incubated with antibodies at different times, the signal intensity in the control sample for each blot was set to 1.0 (to permit collective analysis) and significance was determined by one-sample *t*-test.

Results

WT SMCs acutely expressing progerin display contractile characteristics of HGPS

As HGPS is a very rare disease, the understanding of its molecular pathology has relied heavily on the use of mouse models. Osorio *et al.* generated a knock-in mouse ($Lmna^{G609G}$; hereafter called the HGPS mouse) that contains the equivalent point mutation to the G608G

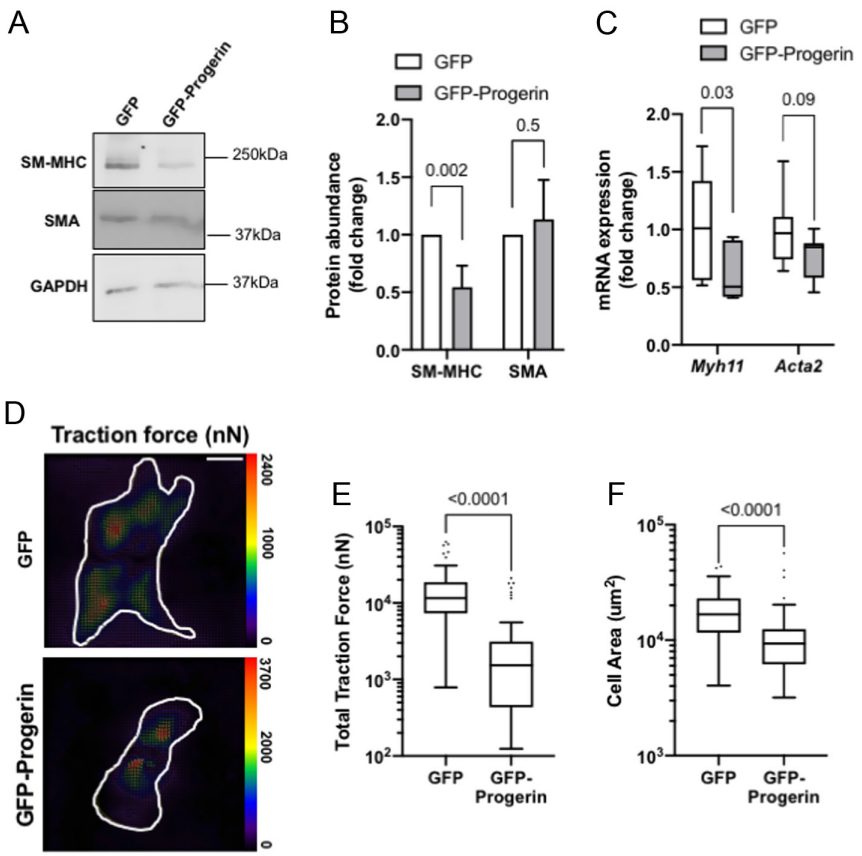

Figure 1
Acute progerin expression in WT SMCs phenocopies the contractile defects in HGPS SMCs. Vascular SMCs isolated from 2-month WT mouse aortas were incubated with adenoviruses encoding GFP (control) or GFP-progerin for 72 h. (A) Representative immunoblot images of smMHC (n = 6) and SMA (n = 4) protein abundance. GAPDH is shown as the loading control. (B) Results in A were quantified and normalized to the loading control. As independent experiments were fractionated and blotted separately, the normalized signal in the GFP-infected cells of each blot was defined as 1.0 to permit collective presentation and analysis of the data. Results show mean + s.d. Statistical significance between the cells infected with GFP or GFP-progerin was determined by one-sample *t*-test (see 'Statistical analysis' section in 'Materials and methods' section). (C) WT SMCs infected with the GFP and GFP-progerin adenoviruses were analyzed for the expression of *Myh11* and *Acta2* mRNA levels by RT-qPCR (n = 7–8). Results are presented as box plots with Tukey whiskers. Statistical significance was determined by Mann–Whitney test. (D) Representative traction force images of WT SMCs infected with the GFP and GFP-progerin adenoviruses. Cell areas are outlined in white, and traction force scale bars (in nanonewtons) are displayed to the right of each respective image. Optical scale bar = 50 μm. (E and F) Quantification of total traction forces and cell areas of the infected cells displayed as box plots with Tukey whiskers (n = 60–70 cells accrued from three independent experiments). Significance in panels (E) and (F) was determined by Mann–Whitney tests.

https://vb.bioscientifica.com
https://doi.org/10.1530/VB-21-0018
© 2022 The authors
Published by Bioscientifica Ltd

This work is licensed under a Creative Commons Attribution-NonCommercial 4.0 International License.

mutation seen in human HGPS (42). As stated above, the levels of smMHC are reduced in arteries and early passage SMCs isolated from these mice, and this effect is functionally significant: RNAi-mediated knockdown of *Myh11* in cultured WT SMCs reproduced the reductions in cell area and traction force seen in HGPS SMCs while overexpression of smMHC restored traction force in HGPS SMCs (38).

To determine whether these effects are direct consequences of progerin expression or long-term adaptive responses, we acutely infected early passage SMCs isolated from WT mice with a progerin adenovirus tagged with a green fluorescent protein (GFP) or a GFP adenovirus as control. Indeed, we found that acute expression of GFP-progerin reduced smMHC (Fig. 1A, B and Supplementary Fig. 1A, see section on supplementary materials given at the end of this article) and *Myh11* mRNA (Fig. 1C) levels, total traction force (Fig. 1D and E), and cell area (Fig. 1D and F) relative to the GFP control. Acute progerin expression even reproduced the stronger reduction in *Myh11* mRNA and smMHC protein abundance as compared to *Acta2* mRNA and SMA protein (Fig. 1A, B and C) that characterizes HGPS SMCs (38).

In an effort to identify a possible mechanism with *in vivo* relevance, we interrogated our recent transcriptome-wide analysis of aortas isolated from 2-month-old WT vs HGPS mice (GEO dataset GSE165409) and identified ~2800 differentially expressed genes (DEGs) (Fig. 2A and Supplementary Table 1). Analysis of this dataset confirmed reduced mRNA expression for *Myh11* mRNA and other contractile smooth muscle markers (Supplementary Fig. 2; red) as well as increased mRNA expression of SMC synthetic markers (Supplementary Fig. 2; green). We then used IPA to interrogate transcriptional regulator signatures within these ~2800 DEGs and identified 98 transcriptional regulators predicted to be differentially activated or inhibited in the HGPS aortas (Fig. 2A and Supplementary Table 2). Of these, seven included *Myh11* in their target gene lists (Fig. 2A and red or green type in Supplementary Table 2), and only three of these were predicted to be inhibited in HGPS (Fig. 2A and red type in Supplementary Table 2). Two of these inhibited transcription regulators were SRF and MRTF-A, the canonical regulators of contractile gene expression; the third was FOXA1 (Fig. 2B). Note that the signature for myocardin was not strongly inhibited in HGPS aortas (Fig. 2B and Supplementary Table 2).

We did not pursue FOXA1 given that it is typically expressed in endodermally derived (rather than mesenchymally derived) tissue and is not among the *Fox* genes that have been strongly implicated in vascular disease (43, 44). Moreover and consistent with this literature, the expression of *Foxa1* mRNA was barely detected in the RNASeq (average normalized counts in WT and HGPS aortas = 0.13 and 0, respectively; $n = 6$ per genotype). In contrast, we were particularly interested in MRTF-A given its established regulation by changes in cell mechanics (33, 34, 35) as we see in HGPS SMCs (Fig. 1 and (38)). Moreover, and consistent with the notion of MRTF-A regulation by subcellular localization, we found that MRTF-A abundance was similar in lysates of 2-month WT and HGPS aortas (Fig. 2C, D and Supplementary Fig. 1B) despite the difference in its transcriptional signature (Fig. 2B).

A reduced MRTF-A nuclear–cytoplasmic ratio in HGPS SMCs is phenocopied by acute progerin expression

Since early passage HGPS SMCs phenocopy the reduced expression of *Myh11* mRNA and smMHC seen in the HGPS

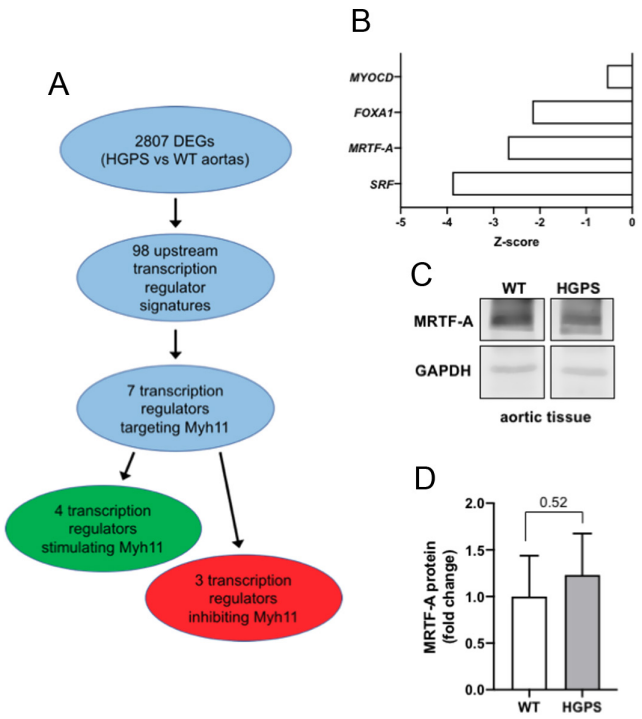

Figure 2
Reduced MRTF signature in HGPS aortas. (A) Overview of bioinformatic analysis using Ingenuity Pathway Analysis. (B) Z-scores of the three transcription factor signatures (FOXA1, MRTF-A, and SRF) predicted from the bioinformatic analysis in A and including myocardin (MYOCD) as reference. (C) Representative immunoblot images of MRTF-A levels in descending aortas of 2-month WT (n = 3) and HGPS (n = 4) mice with GAPDH shown as the loading control. (D) Results in (C) were quantified, normalized to the loading control for each sample, and plotted as mean + S.D. As all replicates were fractionated and immunoblotted together; statistical significance was determined by unpaired t-test.

https://vb.bioscientifica.com
https://doi.org/10.1530/VB-21-0018
© 2022 The authors
Published by Bioscientifica Ltd

This work is licensed under a Creative Commons Attribution-NonCommercial 4.0 International License.

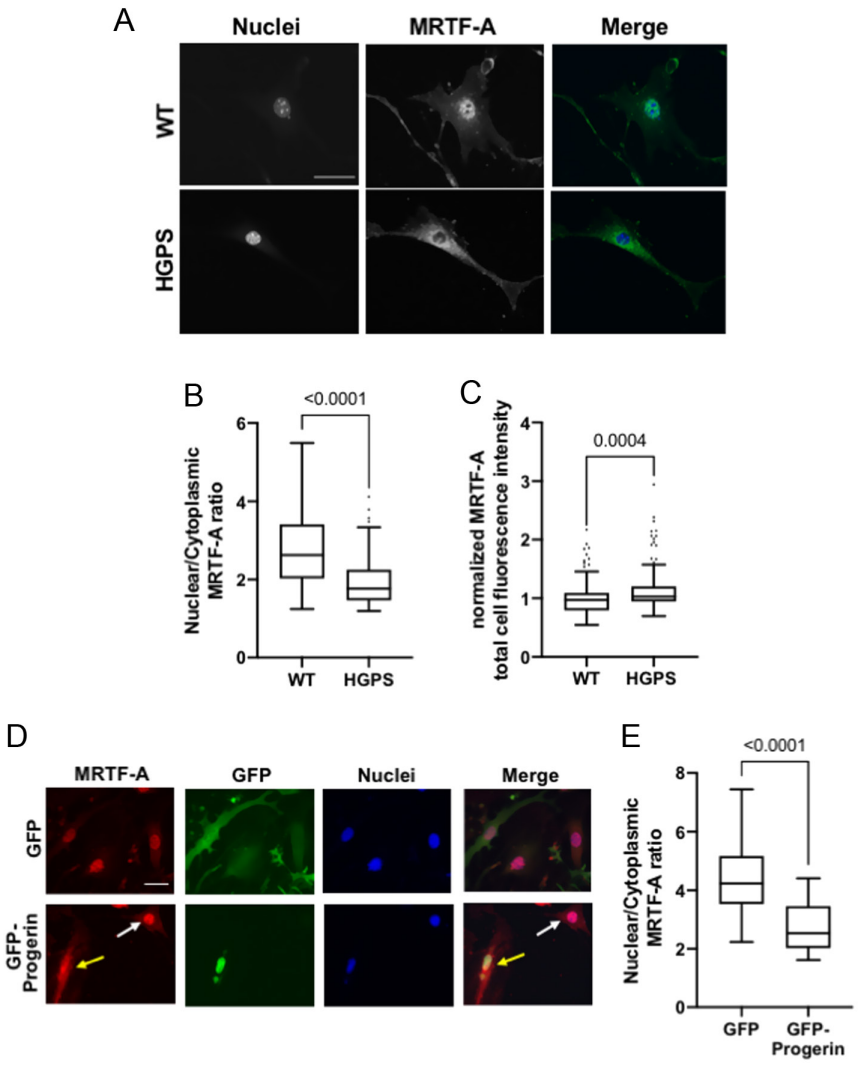

Figure 3
Reduced nuclear MRTF-A in HGPS SMCs phenocopied by acute expression of progerin. (A, B, and C) Early passage SMCs isolated from the descending aortas of 2-month male WT and HGPS mice were immunostained for MRTF-A and counterstained with Dapi to identify nuclei. (B and C) Nuclear–cytoplasmic MRTF-A ratios and total cellular levels of MRTF-A, respectively, were determined from ~120 to 150 cells accrued from four independent experiments. Data are displayed as box plots with Tukey whiskers, and statistical significance was determined by Mann–Whitney tests. (D) Representative images of WT SMCs incubated with adenoviruses encoding GFP or GFP-progerin for 72 h. Collected coverslips were immunostained for MRTF-A and counterstained with Dapi. The yellow and white arrows in the bottom panels point to the nucleus in a progerin-infected and a progerin-uninfected cell, respectively. Scale bar = 50 μm. (E) Quantification of nuclear–cytoplasmic ratios of WT and HGPS SMCs infected with adenoviruses encoding GFP or GFP-progerin (n = ~35 to 50 cells accrued from two independent experiments). Data are displayed as box plots with Tukey whiskers, and significance was determined by a Mann–Whitney test.

aorta (refer to Fig. 1 and (38)), we used these cells to assess the effect of progerin on MRTF localization. HGPS SMCs had a significantly reduced nuclear–cytoplasmic ratio of MRTF-A as compared to WT controls (Fig. 3A and B). Consistent with our results in aortas (refer to Fig. 2), total levels of MRTF-A were similar, if not slightly higher, in WT and HGPS SMCs (Fig. 3C).

We then acutely infected WT SMCs with adenoviruses encoding either GFP-progerin (Fig. 3D bottom panels) or the GFP control (Fig. 3D top panels) and observed that the progerin-expressing cells (Fig. 3D bottom panels, yellow arrows) displayed diffuse MRTF-A staining as compared to the predominantly nuclear staining seen in the SMCs that remained uninfected (Fig. 3D bottom panels, white arrows) and in the SMC infected with the adeno-GFP control (Fig. 3D top panels). Quantification of these differences showed high statistical significance (Fig. 3E). Thus, we conclude that the reduced nuclear MRTF-A in HGPS SMCs is a direct consequence of progerin expression.

Knockdown of MRTF-A in WT SMCs with three distinct siRNAs (Fig. 4A, B and Supplementary Fig. 1C) strongly reduced expression of *Myh11* mRNA (Fig. 4C). Moreover, the effect of MRTF-A depletion on *Myh11* mRNA was more pronounced than the effect on *Acta2* mRNA (Fig. 4C) and thereby resembled the relative differences in smMHC and SMA protein levels that we have observed in HGPS SMCs (38).

The effect of progerin on contractile genes is independent of the LINC complex

Others have reported that disruption of the LINC complex reduces the effect of progerin on cell death in cultured HGPS SMCs and loss of medial aortic SMCs in HGPS mice (17). To determine if disruption of the LINC complex might also

https://vb.bioscientifica.com
https://doi.org/10.1530/VB-21-0018
© 2022 The authors
Published by Bioscientifica Ltd

This work is licensed under a Creative Commons Attribution-NonCommercial 4.0 International License.

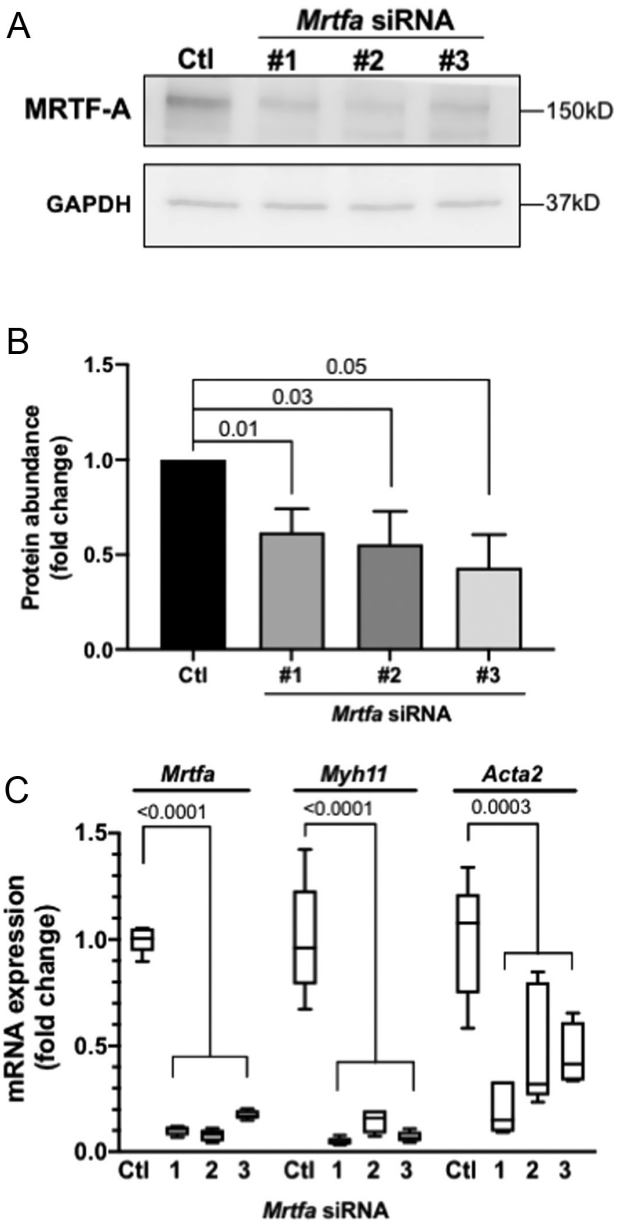

Figure 4

MRTF-A knockdown in WT SMCs phenocopies the preferential downregulation of *Myh11* mRNA in HGPS. WT SMCs were incubated with a non-specific (control) siRNA or three distinct siRNAs to MRTF-A for 72 h. (A) Representative immunoblot images showing MRTF-A levels in the control and the cells treated with MRTF-A siRNA #1–3. GAPDH is shown as the loading control. (B) Results in (A) were quantified and normalized to the loading control. As independent experiments were fractionated and blotted separately, the normalized signal in the control siRNA of each blot was defined as 1.0 to permit collective presentation and analysis of the data. Results show mean + S.D. (n =3). Statistical significance between the control and each MRTF-A siRNA was determined by one-sample t-test (see 'Statistical analysis' section in 'Materials and methods' section). (C) mRNA levels for smooth muscle contractile genes were determined by RT-qPCR and normalized to the control siRNA. Results are displayed as box plots with Tukey whiskers (n = 5). Statistical significance between the cells transfected with control siRNA and each MRTF-A siRNA was determined by ANOVA for each transcript.

improve contractile gene expression in HGPS, we infected WT and HGPS SMCs with a Klarsicht, ANC-1, Syne homology (KASH) domain-encoding lentivirus tagged with GFP (or a GFP lentivirus as control). While overexpression of GFP-KASH effectively disrupted the nuclear membrane as judged by the displacement of endogenous nesprins from the nuclear envelope, the aberrantly low expression levels of these contractile genes in HGPS SMCs were not improved by KASH expression (Supplementary Fig. 3).

Discussion

In this work, we show that acute progerin expression recapitulates the decrease in smMHC protein and *Myh11* mRNA that we previously observed in HGPS aortas, carotids, and cultured SMCs (38). The *Myh11* gene contains CArG sites and is regulated by SRF and the cytoplasmic-nuclear shuttling of MRTFs (see 'Introduction' section). Our bioinformatic analysis of isolated WT 'and HGPS aortas predicted a decrease in SRF and MRTF signatures in HGPS that could explain the decreased expression of *Myh11* mRNA and smMHC protein. Consistent with that prediction, we found a decrease in the nuclear abundance of MRTF-A in isolated HGPS SMCs relative to WT controls. Acute progerin expression in WT SMCs recapitulated the low levels of nuclear MRTF-A seen in HGPS SMCs indicating the effect of progerin on MRTF localization, as well as smMHC abundance, is a direct rather than long-term adaptive effect.

Although *Myh11* and *Acta2* are both CArG genes and markers of differentiated smooth muscle, our previous work (38) and this report show that the expression of progerin has a stronger inhibitory effect on the expression of *Myh11* mRNA than *Acta2* mRNA. Other CArG genes such as *Tagln* and *Cnn1* behave more like *Acta2*, as the expression levels of their mRNAs are also relatively resistant to the expression progerin (38). This difference may reflect a greater number of CArG sites in the *Myh11* vs *Acta2* genes, increased relative potency of the CArG sites in *Myh11* relative to other SMC contractile genes, and perhaps even distinct post-transcriptional effects of progerin on mRNA stability. Progerin might also affect the regulatory phosphorylation of MRTFs or the epigenetic landscape (45, 46, 47). Surprisingly, we found that the effect of progerin on *Myh11* gene expression was resistant to disruption of the LINC complex. A fuller understanding of progerin's effect on MRTF nuclear localization and CArG gene expression and how these effects preferentially target *Myh11* vs *Acta2* independent of the LINC complex are important matters for further study.

https://vb.bioscientifica.com
https://doi.org/10.1530/VB-21-0018
© 2022 The authors
Published by Bioscientifica Ltd

This work is licensed under a Creative Commons Attribution-NonCommercial 4.0 International License.

In addition to displaying decreased expression of *Myh11* and other smooth muscle differentiation markers, arteries and SMCs from HGPS mice show reduced contractility and increased production and remodeling of the ECM (38, 41, 48, 49, 50, 51). Our analysis of DEGs in HGPS also revealed an increased gene expression of 'synthetic' SMC markers in HGPS aortas. Collectively, these results lead us to posit that HGPS SMCs exist in a relatively de-differentiated phenotypic state. This idea is further supported by our finding of a reduced average size of HGPS SMCs, as de-differentiated SMCs are smaller than differentiated ones (38, 52). A defect in vascular smooth muscle differentiation, in turn, might contribute to ECM remodeling, vascular fibrosis, and the increased stiffness seen in the arteries of HGPS children (53).

Death in HGPS is most commonly due to heart attack or stroke, but the range of symptoms in HGPS extends well beyond vascular disease and includes alopecia, stunted growth, low bone density, loss of subcutaneous fat, reduced hearing, altered dentition, extra-skeletal calcification, left ventricular hypertrophy, and diastolic dysfunction (3, 50, 54, 55, 56, 57). In a recent study, we linked diastolic dysfunction in HGPS to arterial and/or cardiac stiffness (41), but overall the basis for the complex pathology of HGPS remains incompletely understood. It is tempting to speculate that a defective arterial MRTF-*Myh11* pathway as described here may compromise blood flow and thereby contribute systemically to some of the diverse defects in HGPS. Experimental testing of this hypothesis would be an important matter for further study.

Supplementary materials

This is linked to the online version of the paper at https://doi.org/10.1530/VB-21-0018.

Declaration of interest

The authors declare that there is no conflict of interest that could be perceived as prejudicing the impartiality of the research reported.

Funding

This work was supported by NIH grant AG062140 to R K A and by the Center for MechanoBiology, a National Science Foundation Science and Technology Center under grant agreement CMMI 15-48571. R v K was supported by NIH grants T32-GM008076 and F31-HL142160.

Author contribution statement

Experiments were designed by R v K and R K A and performed by R v K and P C. R v K and R K A performed the data analysis, statistical testing, and prepared the manuscript text and figures.

Acknowledgements

The authors thank Carlos Lopez-Otin (Universidad de Oviedo, Oviedo, Spain) for the LMNA^{G609G} mice and Gregg Gundersen (Columbia University) for the lentiviruses and nesprin-2 antibody.

References

1 Sinha JK, Ghosh S & Raghunath M. Progeria: a rare genetic premature ageing disorder. *Indian Journal of Medical Research* 2014 **139** 667–674.
2 Saxena S & Kumar S. Pharmacotherapy to gene editing: potential therapeutic approaches for Hutchinson–Gilford progeria syndrome. *GeroScience* 2020 **42** 467–494. (https://doi.org/10.1007/s11357-020-00167-3)
3 Merideth MA, Gordon LB, Clauss S, Sachdev V, Smith ACM, Perry MB, Brewer CC, Zalewski C, Kim HJ, Solomon B, *et al*. Phenotype and course of Hutchinson–Gilford progeria syndrome. *New England Journal of Medicine* 2008 **358** 592–604. (https://doi.org/10.1056/NEJMoa0706898)
4 De Sandre-Giovannoli A, Bernard R, Cau P, Navarro C, Amiel J, Boccaccio I, Lyonnet S, Stewart CL, Munnich A, Le Merrer M, *et al*. Lamin A truncation in Hutchinson–Gilford progeria. *Science* 2003 **300** 2055. (https://doi.org/10.1126/science.1084125)
5 Eriksson M, Brown WT, Gordon LB, Glynn MW, Singer J, Scott L, Erdos MR, Robbins CM, Moses TY, Berglund P, *et al*. Recurrent de novo point mutations in lamin A cause Hutchinson–Gilford progeria syndrome. *Nature* 2003 **423** 293–298. (https://doi.org/10.1038/nature01629)
6 Goldman RD, Shumaker DK, Erdos MR, Eriksson M, Goldman AE, Gordon LB, Gruenbaum Y, Khuon S, Mendez M, Varga R, *et al*. Accumulation of mutant lamin A progressive changes in nuclear architecture in Hutchinson–Gilford progeria syndrome. *PNAS* 2004 **101** 8963–8968. (https://doi.org/10.1073/pnas.0402943101)
7 Dahl KN, Scaffidi P, Islam MF, Yodh AG, Wilson KL & Misteli T. Distinct structural and mechanical properties of the nuclear lamina in Hutchinson–Gilford progeria syndrome. *PNAS* 2006 **103** 10271–10276. (https://doi.org/10.1073/pnas.0601058103)
8 Kelley JB, Datta S, Snow CJ, Chatterjee M, Ni L, Spencer A, Yang CS, Cubeñas-Potts C, Matunis MJ & Paschal BM. The defective nuclear lamina in Hutchinson–Gilford progeria syndrome disrupts the nucleocytoplasmic Ran gradient and inhibits nuclear localization of Ubc9. *Molecular and Cellular Biology* 2011 **31** 3378–3395. (https://doi.org/10.1128/MCB.05087-11)
9 Hamczyk MR, del Campo L & Andrés V. Aging in the cardiovascular system: lessons from Hutchinson–Gilford progeria syndrome. *Annual Review of Physiology* 2018 **80** 27–48. (https://doi.org/10.1146/annurev-physiol-021317-121454)
10 Lombardi ML & Lammerding J. Keeping the LINC: the importance of nucleocytoskeletal coupling in intracellular force transmission and cellular function. *Biochemical Society Transactions* 2011 **39** 1729–1734. (https://doi.org/10.1042/BST20110686)
11 Chang W, Worman HJ & Gundersen GG. Accessorizing and anchoring the LINC complex for multifunctionality. *Journal of Cell Biology* 2015 **208** 11–22. (https://doi.org/10.1083/jcb.201409047)
12 Dahl KN, Ribeiro AJS & Lammerding J. Nuclear shape, mechanics, and mechanotransduction. *Circulation Research* 2008 **102** 1307–1318. (https://doi.org/10.1161/CIRCRESAHA.108.173989)
13 Crisp M, Liu Q, Roux K, Rattner JB, Shanahan C, Burke B, Stahl PD & Hodzic D. Coupling of the nucleus and cytoplasm: role of the LINC complex. *Journal of Cell Biology* 2006 **172** 41–53. (https://doi.org/10.1083/jcb.200509124)
14 Martino F, Perestrelo AR, Vinarský V, Pagliari S & Forte G. Cellular mechanotransduction: from tension to function. *Frontiers in Physiology* 2018 **9** 824. (https://doi.org/10.3389/fphys.2018.00824)

© 2022 The authors
Published by Bioscientifica Ltd

This work is licensed under a Creative Commons Attribution-NonCommercial 4.0 International License.

15 Chang W, Wang Y, Gant Luxton GWG, Östlund C, Worman HJ & Gundersen GG. Imbalanced nucleocytoskeletal connections create common polarity defects in progeria and physiological aging. *PNAS* 2019 **116** 3578–3583. (https://doi.org/10.1073/pnas.1809683116)

16 Verstraeten VLRM, Ji JY, Cummings KS, Lee RT & Lammerding J. Increased mechanosensitivity and nuclear stiffness in Hutchinson–Gilford progeria cells: effects of farnesyltransferase inhibitors. *Aging Cell* 2008 **7** 383–393. (https://doi.org/10.1111/j.1474-9726.2008.00382.x)

17 Kim PH, Luu J, Heizer P, Tu Y, Weston TA, Chen N, Lim C, Li RL, Lin PY, Dunn JCY, *et al*. Disrupting the LINC complex in smooth muscle cells reduces aortic disease in a mouse model of Hutchinson–Gilford progeria syndrome. *Science Translational Medicine* 2018 **10** eaat7163. (https://doi.org/10.1126/scitranslmed.aat7163)

18 Yoshida T & Owens GK. Molecular determinants of vascular smooth muscle cell diversity. *Circulation Research* 2005 **96** 280–291. (https://doi.org/10.1161/01.RES.0000155951.62152.2e)

19 Beamish JA, He P, Kottke-Marchant K & Marchant RE. Molecular regulation of contractile smooth muscle cell phenotype: implications for vascular tissue engineering. *Tissue Engineering: Part B, Reviews* 2010 **16** 467–491. (https://doi.org/10.1089/ten.TEB.2009.0630)

20 Rensen SSM, Doevendans PAFM & Van Eys GJJM. Regulation and characteristics of vascular smooth muscle cell phenotypic diversity. *Netherlands Heart Journal* 2007 **15** 100–108. (https://doi.org/10.1007/BF03085963)

21 Owens GK, Kumar MS & Wamhoff BR. Molecular regulation of vascular smooth muscle cell differentiation in development and disease. *Physiological Reviews* 2004 **84** 767–801. (https://doi.org/10.1152/physrev.00041.2003)

22 Thyberg J, Blomgren K, Roy J, Tran PK & Hedin U. Phenotypic modulation of smooth muscle cells after arterial injury is associated with changes in the distribution of laminin and fibronectin. *Journal of Histochemistry and Cytochemistry* 1997 **45** 837–846. (https://doi.org/10.1177/002215549704500608)

23 Zhang SM, Zhu LH, Chen HZ, Zhang R, Zhang P, Jiang DS, Gao L, Tian S, Wang L, Zhang Y, *et al*. Interferon regulatory factor 9 is critical for neointima formation following vascular injury. *Nature Communications* 2014 **5** 5160. (https://doi.org/10.1038/ncomms6160)

24 Grootaert MOJ & Bennett MR. Vascular smooth muscle cells in atherosclerosis: time for a re-assessment. *Cardiovascular Research* 2021 **117** 2326–2339. (https://doi.org/10.1093/cvr/cvab046)

25 Hao H, Gabbiani G & Bochaton-Piallat ML. Arterial smooth muscle cell heterogeneity: implications for atherosclerosis and restenosis development. *Arteriosclerosis, Thrombosis, and Vascular Biology* 2003 **23** 1510–1520. (https://doi.org/10.1161/01.ATV.0000090130.85752.ED)

26 Migdalski A & Jawien A. New insight into biology, molecular diagnostics and treatment options of unstable carotid atherosclerotic plaque: a narrative review. *Annals of Translational Medicine* 2021 **9** 1207–1207. (https://doi.org/10.21037/atm-20-7197)

27 Olson EN & Nordheim A. Linking actin dynamics and gene transcription to drive cellular motile functions. *Nature Reviews: Molecular Cell Biology* 2010 **11** 353–365. (https://doi.org/10.1038/nrm2890)

28 Madsen CS, Regan CP, Hungerford JE, White SL, Manabe I & Owens GK. Smooth muscle-specific expression of the smooth muscle myosin heavy chain gene in transgenic mice requires 5′-flanking and first intronic DNA sequence. *Circulation Research* 1998 **82** 908–917. (https://doi.org/10.1161/01.res.82.8.908)

29 Manabe I & Owens GK. CArG elements control smooth muscle subtype-specific expression of smooth muscle myosin in vivo. *Journal of Clinical Investigation* 2001 **107** 823–834. (https://doi.org/10.1172/JCI11385)

30 Gomez D & Owens GK. Smooth muscle cell phenotypic switching in atherosclerosis. *Cardiovascular Research* 2012 **95** 156–164. (https://doi.org/10.1093/cvr/cvs115)

31 Miano JM. Serum response factor: toggling between disparate programs of gene expression. *Journal of Molecular and Cellular Cardiology* 2003 **35** 577–593. (https://doi.org/10.1016/s0022-2828(03)00110-x)

32 Pipes GCCT, Creemers EE & Olson EN. The myocardin family of transcriptional coactivators: versatile regulators of cell growth, migration, and myogenesis. *Genes and Development* 2006 **20** 1545–1556. (https://doi.org/10.1101/gad.1428006)

33 Miralles F, Posern G, Zaromytidou AI & Treisman R. Actin dynamics control SRF activity by regulation of its coactivator MAL. *Cell* 2003 **113** 329–342. (https://doi.org/10.1016/s0092-8674(03)00278-2)

34 Guettler S, Vartiainen MK, Miralles F, Larijani B & Treisman R. RPEL motifs link the serum response factor cofactor MAL but not myocardin to Rho signaling via actin binding. *Molecular and Cellular Biology* 2008 **28** 732–742. (https://doi.org/10.1128/MCB.01623-07)

35 Montel L, Sotiropoulos A & Hénon S. The nature and intensity of mechanical stimulation drive different dynamics of MRTF-A nuclear redistribution after actin remodeling in myoblasts. *PLoS ONE* 2019 **14** e0214385. (https://doi.org/10.1371/journal.pone.0214385)

36 McDonald OG, Wamhoff BR, Hoofnagle MH & Owens GK. Control of SRF binding to CArG box chromatin regulates smooth muscle gene expression in vivo. *Journal of Clinical Investigation* 2006 **116** 36–48. (https://doi.org/10.1172/JCI26505)

37 Gomez D, Swiatlowska P & Owens GK. Epigenetic control of smooth muscle cell identity and lineage memory. *Arteriosclerosis, Thrombosis, and Vascular Biology* 2015 **35** 2508–2516. (https://doi.org/10.1161/ATVBAHA.115.305044)

38 von Kleeck R, Castagnino P, Roberts E, Talwar S, Ferrari G & Assoian RK. Decreased vascular smooth muscle contractility in Hutchinson–Gilford progeria syndrome linked to defective smooth muscle myosin heavy chain expression. *Scientific Reports* 2021 **11** 10625. (https://doi.org/10.1038/s41598-021-90119-4)

39 Cuff CA, Kothapalli D, Azonobi I, Chun S, Zhang Y, Belkin R, Yeh C, Secreto A, Assoian RK, Rader DJ, *et al*. The adhesion receptor CD44 promotes atherosclerosis by mediating inflammatory cell recruitment and vascular cell activation. *Journal of Clinical Investigation* 2001 **108** 1031–1040. (https://doi.org/10.1172/JCI12455)

40 Zhang Q, Narayanan V, Mui KL, O'Bryan CS, Anderson RH, Kc B, Cabe JI, Denis KB, Antoku S, Roux KJ, *et al*. Mechanical stabilization of the glandular acinus by linker of nucleoskeleton and cytoskeleton complex. *Current Biology* 2019 **29** 2826.e4–2839.e4. (https://doi.org/10.1016/j.cub.2019.07.021)

41 von Kleeck R, Roberts E, Castagnino P, Bruun K, Brankovic SA, Hawthorne EA, Xu T, Tobias JW & Assoian RK. Arterial stiffness and cardiac dysfunction in Hutchinson–Gilford progeria syndrome corrected by inhibition of lysyl oxidase. *Life Science Alliance* 2021 **4** e202000997. (https://doi.org/10.26508/lsa.202000997)

42 Osorio FG, Navarro CL, Cadiñanos J, López-Mejía IC, Quirós PM, Bartoli C, Rivera J, Tazi J, Guzmán G, Varela I, *et al*. Splicing-directed therapy in a new mouse model of human accelerated aging. *Science Translational Medicine* 2011 **3** 106ra107. (https://doi.org/10.1126/scitranslmed.3002847)

43 Yang XF, Fang P, Meng S, Jan M, Xiong X, Yin Y & Wang H. The FOX transcription factors regulate vascular pathology, diabetes and tregs. *Frontiers in Bioscience* 2009 **1** 420–436. (https://doi.org/10.2741/S35)

44 Golson ML & Kaestner KH. Fox transcription factors: from development to disease. *Development* 2016 **143** 4558–4570. (https://doi.org/10.1242/dev.112672)

45 Panayiotou R, Miralles F, Pawlowski R, Diring J, Flynn HR, Skehel M & Treisman R. Phosphorylation acts positively and negatively to regulate MRTF-A subcellular localisation and activity. *eLife* 2016 **5** e15460. (https://doi.org/10.7554/eLife.15460)

46 Köhler F, Bormann F, Raddatz G, Gutekunst J, Corless S, Musch T, Lonsdorf AS, Erhardt S, Lyko F & Rodríguez-Paredes M. Epigenetic deregulation of lamina-associated domains in Hutchinson–Gilford progeria syndrome. *Genome Medicine* 2020 **12** 46. (https://doi.org/10.1186/s13073-020-00749-y)

© 2022 The authors
Published by Bioscientifica Ltd

This work is licensed under a Creative Commons Attribution-NonCommercial 4.0 International License.

47 Arancio W, Pizzolanti G, Genovese SI, Pitrone M & Giordano C. Epigenetic involvement in Hutchinson–Gilford progeria syndrome: a mini-review. *Gerontology* 2014 **60** 197–203. (https://doi.org/10.1159/000357206)
48 del Campo L, Sánchez-López A, Salaices M, von Kleeck RA, Expósito E, González-Gómez C, Cussó L, Guzmán-Martínez G, Ruiz-Cabello J, Desco M, *et al*. Vascular smooth muscle cell-specific progerin expression in a mouse model of Hutchinson–Gilford progeria syndrome promotes arterial stiffness: therapeutic effect of dietary nitrite. *Aging Cell* 2019 **18** e12936. (https://doi.org/10.1111/acel.12936)
49 del Campo L, Sánchez-López A, González-Gómez C, Andrés-Manzano MJ, Dorado B & Andrés V. Vascular smooth muscle cell-specific progerin expression provokes contractile impairment in a mouse model of Hutchinson–Gilford progeria syndrome that is ameliorated by nitrite treatment. *Cells* 2020 **9** 656. (https://doi.org/10.3390/cells9030656)
50 Olive M, Harten I, Mitchell R, Beers JK, Djabali K, Cao K, Erdos MR, Blair C, Funke B, Smoot L, *et al*. Cardiovascular pathology in Hutchinson–Gilford progeria: correlation with the vascular pathology of aging. *Arteriosclerosis, Thrombosis, and Vascular Biology* 2010 **30** 2301–2309. (https://doi.org/10.1161/ATVBAHA.110.209460)
51 Murtada SI, Kawamura Y, Caulk AW, Ahmadzadeh H, Mikush N, Zimmerman K, Kavanagh D, Weiss D, Latorre M, Zhuang ZW, *et al*. Paradoxical aortic stiffening and subsequent cardiac dysfunction in Hutchinson–Gilford progeria syndrome. *Journal of the Royal Society, Interface* 2020 **17** 20200066. (https://doi.org/10.1098/rsif.2020.0066)
52 Talwar S, Kant A, Xu T, Shenoy VB & Assoian RK. Mechanosensitive smooth muscle cell phenotypic plasticity emerging from a null state and the balance between Rac and Rho. *Cell Reports* 2021 **35** 109019. (https://doi.org/10.1016/j.celrep.2021.109019)
53 Gerhard-Herman M, Smoot LB, Wake N, Kieran MW, Kleinman ME, Miller DT, Schwartzman A, Giobbie-Hurder A, Neuberg D & Gordon LB. Mechanisms of premature vascular aging in children with Hutchinson–Gilford progeria syndrome. *Hypertension* 2012 **59** 92–97. (https://doi.org/10.1161/HYPERTENSIONAHA.111.180919)
54 Domingo DL, Trujillo MI, Council SE, Merideth MA, Gordon LB, Wu T, Introne WJ, Gahl WA & Hart TC. Hutchinson–Gilford progeria syndrome: oral and craniofacial phenotypes. *Oral Diseases* 2009 **15** 187–195. (https://doi.org/10.1111/j.1601-0825.2009.01521.x)
55 Gordon CM, Cleveland RH, Baltrusaitis K, Massaro J, D'Agostino RB, Liang MG, Snyder B, Walters M, Li X, Braddock DT, *et al*. Extraskeletal calcifications in Hutchinson–Gilford progeria syndrome. *Bone* 2019 **125** 103–111. (https://doi.org/10.1016/j.bone.2019.05.008)
56 Guardiani E, Zalewski C, Brewer C, Merideth M, Introne W, Smith ACM, Gordon L, Gahl W & Kim HJ. Otologic and audiologic manifestations of Hutchinson–Gilford progeria syndrome. *Laryngoscope* 2011 **121** 2250–2255. (https://doi.org/10.1002/lary.22151)
57 Rork JF, Huang JT, Gordon LB, Kleinman M, Kieran MW & Liang MG. Initial cutaneous manifestations of Hutchinson–Gilford progeria syndrome. *Pediatric Dermatology* 2014 **31** 196–202. (https://doi.org/10.1111/pde.12284)

Received in final form 9 January 2022
Accepted 15 February 2022
Accepted Manuscript published online 15 February 2022

© 2022 The authors
Published by Bioscientifica Ltd

This work is licensed under a Creative Commons Attribution-NonCommercial 4.0 International License.